13th World Conference on Earthquake Engineering
Vancouver, B.C., Canada
August 1-6, 2004
Paper No. 239

INFLUENCE OF HYSTERETIC BEHAVIOR ON THE NONLINEAR RESPONSE OF FRAME STRUCTURES

Ricardo A. MEDINA[1] and Helmut KRAWINKLER[2]

SUMMARY

This paper focuses on understanding and assessing the effect of hysteretic behavior (i.e., bilinear, peak-oriented and pinching) in the evaluation of peak deformation demands and their distribution over the height for regular frame structures over a wide range of stories (from 3 to 18) and fundamental periods (from 0.3 s. to 3.6 s.). The ground motions used are those with frequency content characteristic of ordinary ground motions (no near-fault or soft soil effects). The hysteretic models utilized in this study do not exhibit monotonic or cyclic deterioration; thus, the discussion is most relevant for performance levels related to damage and loss of functionality. Results suggest that the degree of stiffness degradation is important for the seismic performance evaluation of regular frames because systems with a large degree of stiffness degradation tend to exhibit larger peak drift demands and a less uniform distribution of peak drifts over the height. The type of hysteretic behavior also has a significant influence on the dynamic response of long, flexible frames that are prone to global dynamic instability due to P-Delta effects. This study also demonstrates the need to develop reliable procedures to estimate the properties of "equivalent" or "reference" SDOF systems when they are used to evaluate the response of complex MDOF structures with various hysteretic responses at the component level.

INTRODUCTION

Performance evaluation of moment resisting frame structures subject to severe ground shaking requires analytical models able to reasonably represent the cyclic nonlinear behavior of structural components. Numerous studies have dealt with the seismic demand evaluation of systems with various types of hysteretic behavior, e.g., systems with rather stable hysteresis loops and systems that include stiffness degradation typical of reinforced-concrete and timber components. However, most efforts have focused on stiffness degrading SDOF systems, e.g., Rahmana and Krawinkler [1], Oh et. al [2], Song and Pincheira [3], Chung and Loh [4], Miranda and Garcia [5], Farrow and Kurama [6], and there is no consensus regarding the effect of the type of hysteretic response at the component level on the behavior of MDOF systems with and without stiffness degradation.

[1] Assistant Professor, Dept. of Civil and Environmental Engineering, University of Maryland, College Park. Email: ramedina@umd.edu.
[2] Professor, Dept. of Civil and Environmental Engineering, Stanford University, Stanford, CA. Email: krawinkler@stanford.edu.

The objective of this paper is to provide comprehensive information on the influence of hysteretic behavior on the nonlinear response of regular frame structures over a wide range of stories (from 3 to 18) and fundamental periods (from 0.3 sec. to 3.6 sec.). The response parameters used to quantify behavior are the maximum roof drift and the maximum story drift over the height. The ground motions utilized are those with frequency content characteristics of ordinary ground motions. The hysteretic models do not exhibit monotonic or cyclic deterioration; thus, results are most relevant for performance levels related to damage and loss of functionality. A comparison between the nonlinear response of MDOF and SDOF systems with various hysteretic models is presented as well as an evaluation of the effect of the hysteretic model in the probabilistic seismic performance assessment of regular frames.

FRAME MODELS USED IN THIS STUDY

General Description

This study is based on nonlinear time history analyses using twelve two-dimensional, single-bay generic frame models. The generic frame models do not exhibit mass, strength or stiffness irregularities. Results presented by Medina and Krawinkler [7] demonstrate that generic frame models, such as the ones used in this study, are adequate to represent the global dynamic response of more complex regular multi-bay frames. Frame models with number of stories, N, equal to 3, 6, 9, 12, 15, and 18, and a fundamental period, T_1, of $0.1N$ and $0.2N$ are utilized. These T_1 values are deemed to represent lower and upper bound estimates of the fundamental period of regular moment-resisting frames with total heights consistent with the ones used in this research. Frames with a period of $0.1N$ are denoted as "stiff" frames, whereas frames with a period of $0.2N$ are denoted as "flexible" frames.

Properties of Generic Frame Models

The main characteristics of the generic frame models are as follows:

1. The same mass is used at all floor levels
2. Relative stiffnesses are tuned so that the first mode is a straight line (*K1* stiffness pattern)
3. Beam-hinge (*BH*) models are utilized, i.e., plastification only occurs at the end of the beams and the bottom of the first story columns [Fig. 1(a)]
4. Frames are designed so that simultaneous yielding at all plastic hinge locations is attained under a parabolic (NEHRP, $k = 2$) load pattern (*S1* strength pattern)
5. The base shear strength is defined by the parameter $\gamma = V_y/W$ (V_y = base shear yield strength, W = seismically effective weight)
6. Concentrated plasticity is modeled by utilizing nonlinear rotational springs
7. Gravity load moments and the effects of axial column forces on bending strength are not considered
8. Global (structure) P-Delta is included (member P-delta is ignored). The gravity load causing P-Delta effects is taken as the dead load plus a live load equal to 40% of the dead load. The reference value for the P-Delta effect is the elastic first story stability coefficient, $\theta = P_1\delta_{s1}/V_1h_1$, where P_1 is the first story P-Delta gravity load, δ_{s1} and V_1 are the first story drift and shear force, respectively, and h_1 is the first story height
9. For the nonlinear time history analyses, 5% Rayleigh damping is assigned to the first mode and the mode at which the cumulative mass participation exceeds 95%.

HYSTERETIC BEHAVIOR AT PLASTIC HINGE LOCATIONS

Nonlinear behavior at the component level is modeled with a concentrated plasticity approach in which non-deteriorating rotational springs are used to represent the member cyclic response. In this study, three different hysteretic models are used: peak-oriented, bilinear and pinching (Fig. 1). The pinching model corresponds to a severely pinched case in which the coefficients κ_f and κ_d in Fig. 1(d) are equal to 0.25.

The effect of these parameters on the pinching response of the system is illustrated in Fig. 2, which depicts the response of two pinching models with κ_f and κ_d equal to 0.25 and 0.50, respectively. All three models have 3% strain hardening (the post-yield stiffness is 3% of the initial stiffness) and the unloading stiffness is equal to the initial stiffness, i.e., unloading stiffness degradation is not considered.

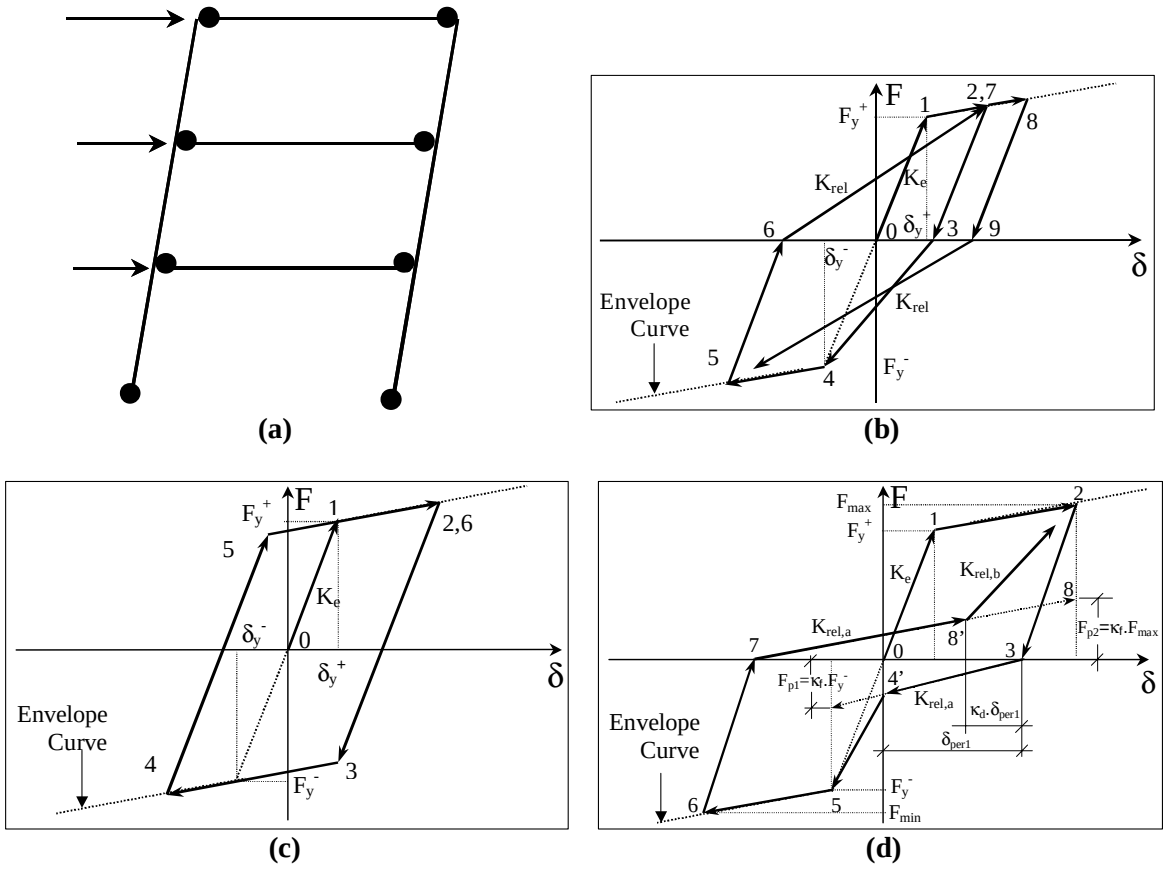

Fig. 1: (a) Beam-hinge mechanism, (b) peak-oriented hysteretic behavior,(c) bilinear hysteretic behavior, (d) pinching hysteretic behavior

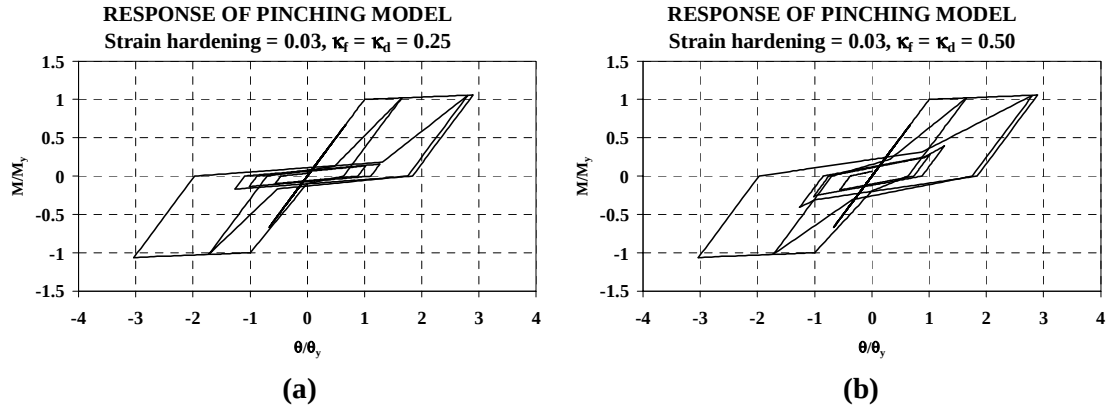

Fig. 2: Various degrees of pinching in the moment-rotation relationship, $\kappa_f = \kappa_d$ = (a) 0.25, (b) 0.50

ORDINARY GROUND MOTIONS

A set of 40 recorded *ordinary* ground motions from Californian earthquakes with moment magnitude between 6.5 and 6.9 and closest distance to the fault rupture between 13 km and 40 km is utilized. In this context, ordinary ground motions refer to those that do not exhibit (a) near-fault, forward-directivity, (b) soft-soil effects, and (c) long-duration effects. This set of ground motions is referred to as "LMSR-N" in subsequent plots. All ground motions were recorded on NEHRP site class D (FEMA [9]). A random horizontal component of ground motion is selected at each station to avoid bias in the selection process. A comprehensive description of the properties of these ground motion records is presented in Ref. [7].

ANALYSIS METHOD

Engineering Demand Parameters

The Engineering Demand Parameters (EDPs) of primary interest are roof and story drifts. As used in this context, the term drift refers to the ratio of relative displacement to the corresponding height, i.e., it defines the tangent of the drift angle, which is equal to the drift angle for the range of interest. The roof drift is considered a measure of the global response (and global damage) of the system while the story drift is assumed to be relevant for structural and non-structural damage assessment as well as global collapse assessment due to dynamic instability caused by P-Delta effects.

Nonlinear Time History Analyses

The basic analysis approach consists of performing nonlinear time history analysis for a given structure and ground motion, using the DRAIN-2DX computer program [10]. The hysteretic models under consideration were incorporated into DRAIN-2DX as new subroutines to carry out this study. For the dynamic analyses, the ground motion intensity is related to the structure strength by the *relative intensity* parameter, $[S_a(T_1)/g]/\gamma$, where $S_a(T_1)$ is the 5% damped spectral acceleration at the fundamental period of the structure, and γ is the base shear coefficient, i.e., $\gamma = V_y/W$. The relative intensity represents the ductility dependent response modification factor (often denoted as R_μ), which is equivalent to the conventional R-factor if no overstrength is present.

The use of $[S_a(T_1)/g]/\gamma$ as a relative intensity measure permits an assessment of the dynamic response of frames based on two different approaches: (a) decreasing the base shear strength of the structure while keeping the ground motion intensity constant (the *R*-factor perspective) and (b) increasing the intensity of the ground motion while keeping the base shear strength constant [the Incremental Dynamic Analysis (IDA) perspective, Vamvatsikos and Cornell [11], see Fig. 13(a)].

Graphical Representation of Results

Two basic graphical communication schemes for a given structure and ground motion are presented. First, graphs of the type shown in Fig. 3 are used. In this case, the relative intensity is plotted on the vertical axis, and the maximum drift is plotted on the horizontal axis. The maximum drift is normalized by the spectral displacement at the first mode period of the system, $S_d(T_1)$, divided by structure height *H*. Second, normalized story drift profile curves are also generated for discrete values of relative intensity (Fig. 4). In this representation, for each structure and ground motion, the number of stories is plotted on the vertical axis and the normalized drift is plotted on the horizontal axis. Data of the type presented in Fig. 4 permits an evaluation of the distribution of story drift over the height of the frames.

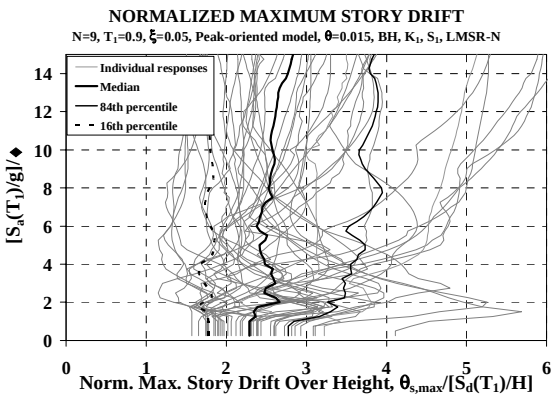

Fig. 3: Normalized max. story drift over the height N = 9, T_1 = 0.9 s., peak-oriented model

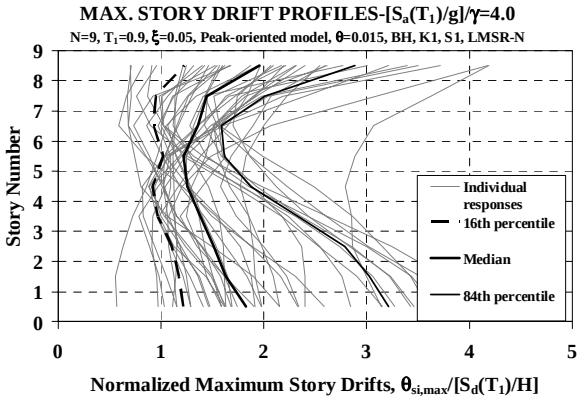

Fig. 4: Normalized max. story drift profiles N = 9, T_1 = 0.9 s., peak-oriented model

If absolute values are of interest, given the ground motion hazard $S_a(T_1)/g$, an appropriate base shear strength can be selected and both the vertical and horizontal axis of Fig. 3 can be de-normalized to obtain their corresponding IDAs. This de-normalization process is illustrated with the data from Fig. 7(b) and Fig. 13, which present the response of a 9-story frame with T_1 = 1.8 seconds in the normalized and IDA domain, respectively. Similarly, given the ground motion hazard and the base shear strength of the structure, graphs of the type presented in Fig. 4 can be used to generate absolute values of the distribution of story drifts over the height.

The second line of the title of the graphs shown in Figs. 3 and 4 corresponds to parameters that have been identified in previous sections. These parameters describe the basic properties of the structural model.

Statistical Representation of Results

The statistical evaluation of results is performed using "counted" statistics, in which values are sorted from smallest to largest, and percentiles are counted rather than computed based on a specific distribution. Counted statistics is needed to evaluate those cases in which data points are lost due to dynamic instability caused by P-Delta effects (i.e., global collapse cases). For consistency, counted statistics is utilized at all relative intensity levels even if the full set of 40 data points is available. Thus, for a set of 40 data points, the median is the average between the 20th and 21st sorted values, the 16th percentile is the average between the 6th and 7th sorted values, and the 84th percentile is the average between the 33rd and 34th sorted values. The standard deviation of the natural logarithm of the data (from here on referred to as dispersion) is estimated by using the counted 16th percentile value, x_{16}. If the counted median is denoted as x_{50}, the dispersion of the data is given by the natural logarithm of the ratio (x_{50} / x_{16}).

EFFECT OF HYSTERETIC BEHAVIOR ON THE NONLINEAR RESPONSE OF FRAMES

The sensitivity of maximum roof and story drifts to the type of hysteretic model is evaluated for the family of twelve generic frame models exposed to the LMSR-N set of ordinary ground motions. In all figures, unless otherwise specified, a pinching model with κ_d = κ_f = 0.25 is utilized and is denoted as "pinching" (the parameters κ_d and κ_f, which control the amount of stiffness degradation in the pinching model, are defined in Fig. 1(d)). A value of 0.25 is chosen because it is representative of severe stiffness degradation in the response.

Maximum Roof and Story Drift Demands

In general, frames with severe pinching (κ_d = κ_f = 0.25) exhibit normalized maximum roof drift demands larger than those observed for the case of frames with peak-oriented and bilinear hysteretic behavior, as

illustrated in Figs. 5 to 7 (which present representative results for the N = 3, 9, and 18 generic frames). Severe stiffness degradation causes the system to become "softer", and hence, experience larger deformation demands. It is important to note that models with peak-oriented hysteretic behavior, which also experience stiffness degradation, exhibit maximum roof drift demands comparable to (and in some cases smaller than) those observed for the bilinear model (except for the frame with T_1 = 0.3 s. in which demands for the peak-oriented model are consistently larger than those experienced by the bilinear model). These observations indicate that for medium to long-period structures, limited stiffness degradation (i.e., peak oriented case) can in some cases "improve" the seismic behavior of regular frame structures. However, when the amount of stiffness degradation is large, it becomes detrimental to the behavior of the system. This pattern is also valid for roof and maximum story drift demands, as the ratio of the two EDPs is essentially independent of the hysteretic model as shown in Fig. 8. This figure depicts the variation of the median ratio of the maximum story drift over the height to the maximum roof drift with the fundamental period of frames, for a relative intensity $[S_a(T_1)/g]/\gamma$ equal to 4.0.

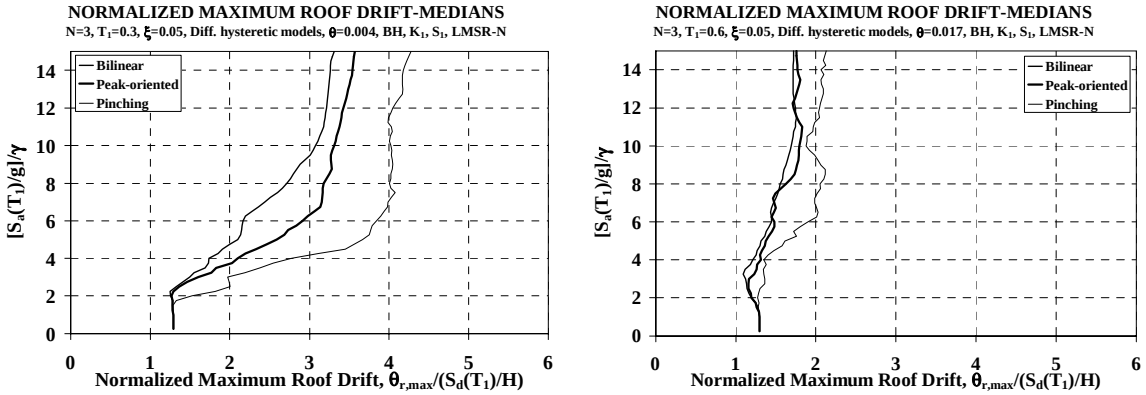

(a) **(b)**

Fig. 5: Median normalized max. roof drift, N = 3, various hysteretic models, T_1 = (a) 0.3 s. and (b) 0.6 s.

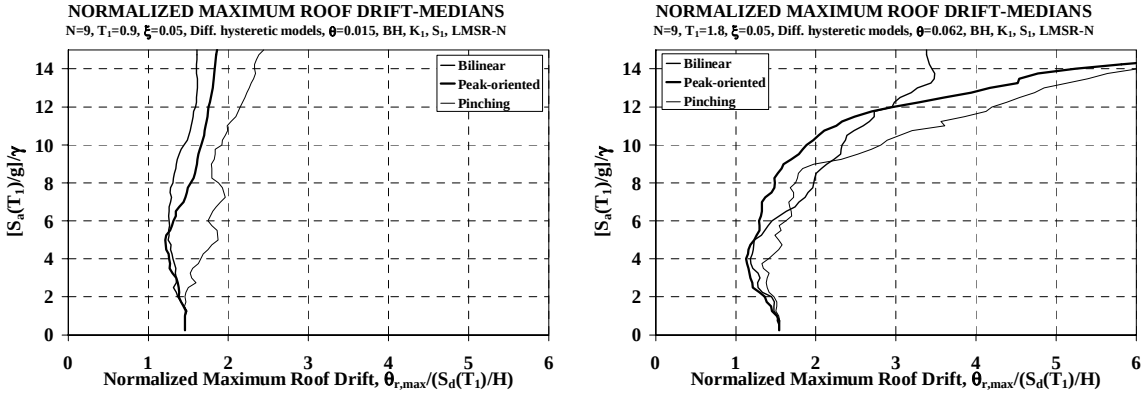

(a) **(b)**

Fig. 6: Median normalized max. roof drift, N = 9, various hysteretic models, T_1 = (a) 0.9 s. and (b) 1.8 s.

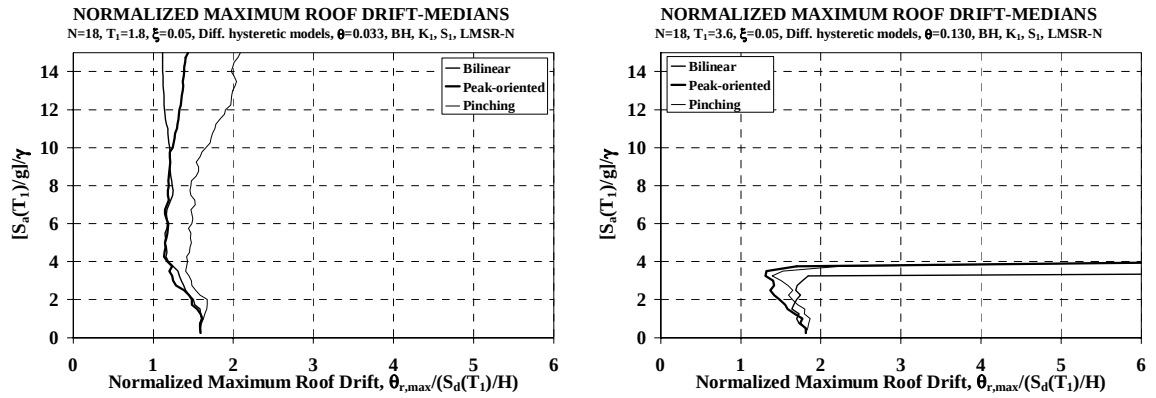

(a) **(b)**

Fig. 7: Median normalized max. roof drift, N = 18, various hysteretic models, T_1 = (a) 1.8 s. and (b) 3.6 s.

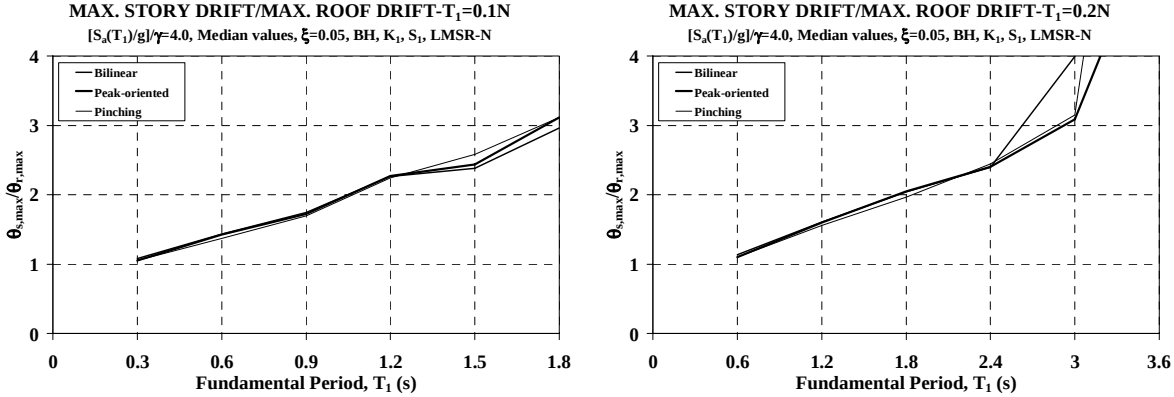

(a) **(b)**

Fig. 8: Median ratio of max. story drift to max. roof drift , $[S_a(T_1)/g]/\gamma$ = 4.0 (a) stiff and (b) flexible frames

P-Delta Effects

The pattern of behavior discussed in the previous paragraph is reversed in the case of flexible structures that are sensitive to P-Delta effects. P-Delta sensitive cases are defined as those in which the effect of gravity loads on the deformed configuration of the system causes large second order effects and, sooner or later, dynamic instability in the response. For these cases [e.g., N = 18, T_1 = 3.6 s., Fig. 7(b)], it is the bilinear model that causes the largest EDPs because the response of the system with bilinear hysteretic behavior spends more time on the envelope of the moment-rotation relationship of its components, which leads to "ratcheting" of the response and potential dynamic instability problems if P-Delta effects produce a negative post-yield tangent stiffness.

Figure 9(a) presents a global pushover curve for the 18-story, T_1 = 3.6 s. frame, which represents the relationship between a global deformation parameter (e.g., roof displacement) and a global strength parameter (e.g., base shear) obtained by subjecting the structure to a predetermined lateral load pattern (in this case a parabolic, NEHRP k = 2 pattern). This pushover curve is common to all hysteretic models since the envelope of the moment-rotation relationship at plastic hinge locations is the same regardless of the type of hysteretic model. Note that for this case the post-yielding tangent stiffness has a large negative value. It is this negative post-yielding tangent stiffness that causes "ratcheting" of the dynamic response (increase in drift in subsequent cycles) and ultimately collapse in a sidesway mode. Such collapse is

observed only if the post-yielding tangent stiffness is negative, and it occurs at a relative intensity that decreases rapidly with an increase in the negative slope of the post-yielding tangent stiffness.

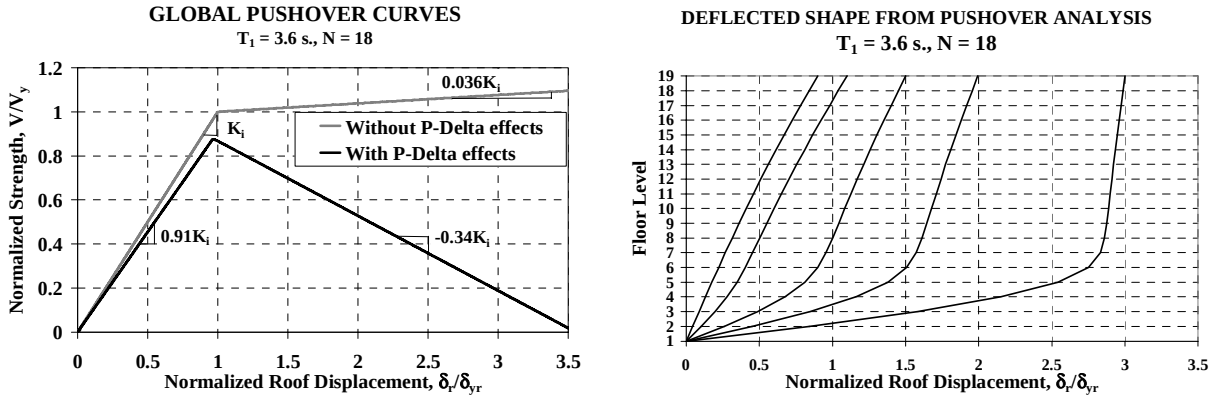

(a) **(b)**

Fig. 9: Pushover analysis, N = 18, T_1 = 3.6 s., (a) global pushover curve, (b) deflected shapes at various levels of roof displacement

Historically, the elastic story stability coefficient, $P\delta/(Vh)$, has been used to quantify the importance of the P-Delta effect. This study and studies performed by others (e.g., Bernal [12], Gupta and Krawinkler [13], and Aydinoglu [14]) have demonstrated that this elastic story stability coefficient may be a poor measure of the importance of P-Delta effects in structures that respond inelastically. A much better measure can be obtained from the global pushover curve. Studies reported in [8] and [15] have shown that a global inelastic stability coefficient, defined as the difference between the post-yielding tangent stiffnesses without and with P-Delta effects of the global pushover curve, and normalized by the elastic stiffness, is a good measure of the importance of P-Delta effect. For the 18-story frame with T_1 = 3.6 s. the elastic global stability coefficient is 0.091, and the inelastic global stability coefficient is 0.376. Thus, the inelastic stability coefficient is more than four times as large as the elastic one. The reason is evident from Fig. 9(b), which shows pushover deflection profiles for this frame. The elastic deflected shape is close to a straight line; however, once the structure yields, there is a concentration of large story drifts in the bottom stories due to the presence of P-Delta effects. As the roof displacement increases, the bottom story drift values increase at a rapid rate until dynamic instability is approached [see curve for δ_r/δ_{yr} = 3.0 in Fig. 9(b)].

Maximum Story Drift Profiles

A more comprehensive picture of the effect of the hysteretic model on the nonlinear response of regular frames can be obtained by studying the distribution of maximum story drifts over the height. Regular frames that exhibit pinching hysteretic behavior at the component level experience a less uniform distribution of maximum story drifts over the height as compared to frames with bilinear and peak-oriented behavior. Differences in the distribution of maximum story drifts over the height are more pronounced at the top and at the bottom of the structure. These observations are illustrated in Fig. 10, which presents median maximum story drift profiles of the 9-story structure with a fundamental period of 0.9 seconds for various values of relative intensity. The general conclusion is that regular frames that have severe pinching in the hysteresis response not only experience the largest roof and story drifts over the height (as presented in previous sections) but also experience the largest amount of total damage (assuming that the maximum story drift is a good indicator of structural and non-structural damage).

These patterns of behavior can have a significant (or at least noteworthy) influence on the seismic performance of existing buildings that will experience significant stiffness degradation when exposed to strong ground shaking, e.g., old reinforced-concrete construction.

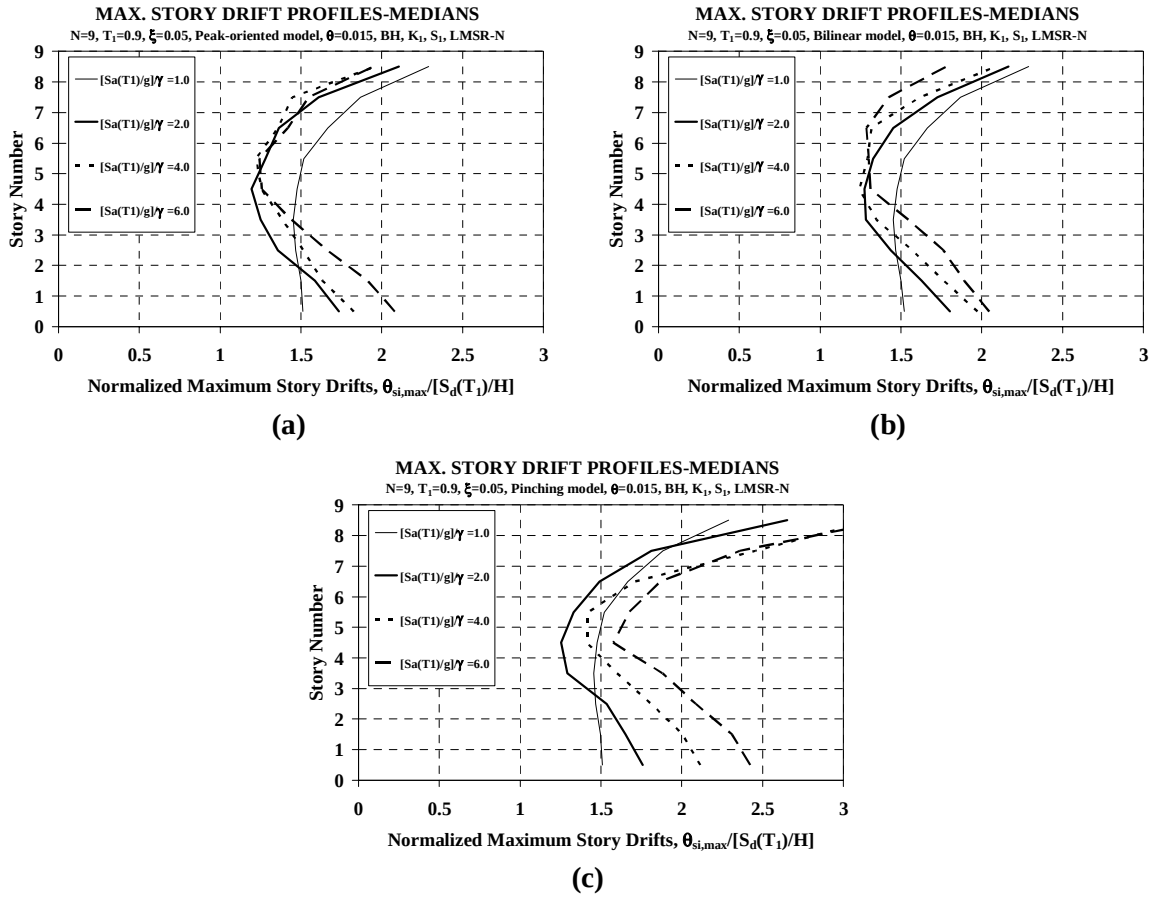

Fig. 10: Median normalized max. story drift profiles, N = 9, T_1 = 0.9 s., various hysteretic models (a) peak-oriented, (b) bilinear, and (c) pinching ($\kappa_d = \kappa_f = 0.25$)

Sensitivity of the Response to the Degree of Stiffness Degradation

The results presented so far suggest that the maximum roof and story drift responses are larger for systems with hysteretic behavior that exhibits severe stiffness degradation such as the pinching model with $\kappa_d = \kappa_f = 0.25$. Unless such severe stiffness degradation is present, the differences between the pinching and peak oriented models are not important as shown in Fig. 11. This figure presents maximum roof drifts for a relative intensity of $[S_a(T_1)/g]/\gamma = 4.0$ for both stiff and flexible frames with hysteretic behavior represented by bilinear, peak-oriented and pinching ($\kappa_d = \kappa_f = 0.25$) models as well as by a pinching model with $\kappa_d = \kappa_f = 0.50$ [denoted in the graphs as "pinching (2)"]. The maximum roof drift demands are similar between the "pinching (2)" (represented by the filled squares in the plot) and peak-oriented models.

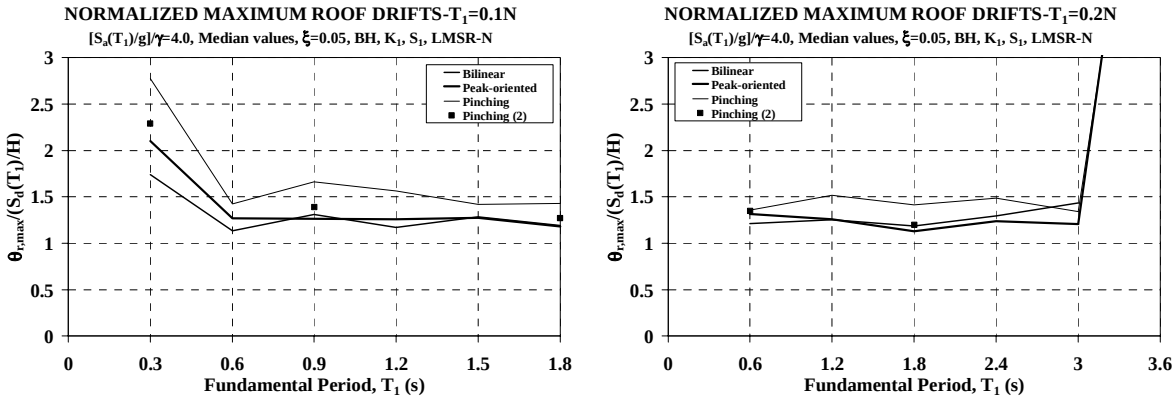

(a) **(b)**

Fig. 11: Median normalized max. roof drift demands, $[S_a(T_1)/g]/\gamma = 4.0$, (a) stiff and (b) flexible frames.

Comparison to SDOF Systems

Fig. 12 presents median ratios of maximum inelastic to elastic displacement for SDOF systems with a strength reduction factor, $R = [S_a(T_1)/g]/\eta$ equal to 4.0, 3% strain hardening, and bilinear, peak-oriented and pinching ($\kappa_d = \kappa_f = 0.25$) hysteretic behavior (the parameter η represents the strength of the SDOF system, which is analogous the MDOF base shear strength parameter, γ). The effect of P-Delta at the SDOF level is represented by rotating the hysteresis diagram by an angle equal to the elastic first story stability coefficient of the 0.1*N* and 0.2*N* frame structures. A comparison of Figs. 11 and 12 shows that except for T = 0.3 s., and except for long period P-Delta sensitive systems, the difference in inelastic displacement demands between the pinching model and the other two models are more pronounced in the MDOF domain. This observation has implications in seismic design and evaluation approaches in which the response of an MDOF system is represented by an "equivalent" SDOF model.

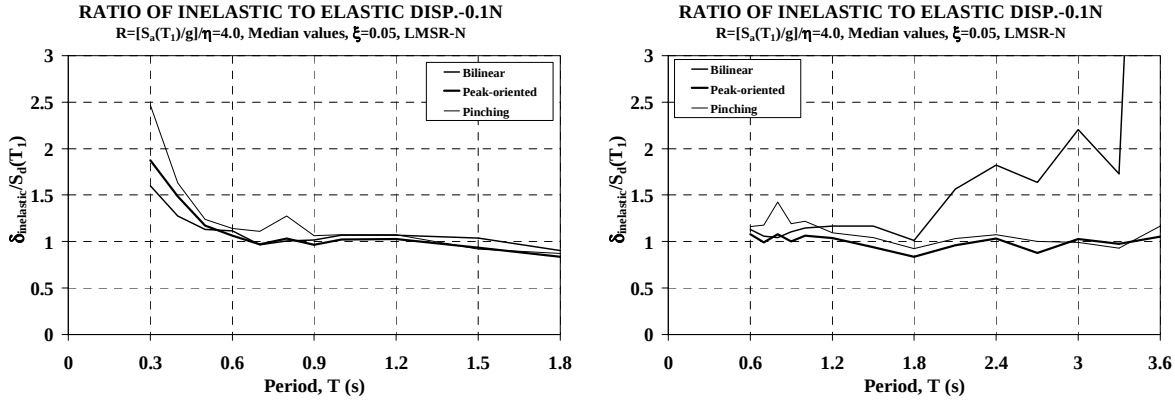

(a) **(b)**

Fig. 12: Median ratio of inelastic to elastic displacement, SDOF systems, various hysteretic models, $R = [S_a(T_1)/g]/\eta = 4.0$ (a) P-Delta slope corresponding to 0.1N and (b) P-Delta slope corresponding to 0.2N

For long period SDOF systems (T > 1.8 s.), the response of the bilinear model becomes P-Delta sensitive while the response of the peak-oriented and pinching models is stable. In this range, the differences between SDOF and MDOF system responses become very large, for reasons discussed in Ref. [15]. Adam et al. [15] present a comprehensive discussion on the use of reference SDOF models to predict global dynamic instability in the response of flexible MDOF frames.

EFFECT OF HYSTERETIC BEHAVIOR ON PROBABILISTIC SEISMIC PERFORMANCE ASSESSMENT

In this section, the implications of differences in the hysteretic behavior on the probabilistic seismic performance assessment of regular frames are illustrated. In this context, performance assessment implies that the structure is given (i.e., $\gamma = V_y/W$, T_1, and other properties are known), and decision variables, such as losses, have to be evaluated (Krawinkler and Miranda [16]). Part of this process is probabilistic seismic demand analysis that includes quantification of engineering demand parameters (*EDPs*) and their associated uncertainties. This quantification can be carried out by computing the mean annual frequency of exceedance of an *EDP*, given by

$$\lambda_{EDP}(y) = \int P\left[EDP \geq y \mid IM = x\right] \left| d\lambda_{IM}(x) \right| \tag{1}$$

where $\lambda_{EDP}(y)$ = mean annual frequency of *EDP* exceeding the value y
$P[EDP \geq y \mid IM = x]$ = probability of *EDP* exceeding y given that *IM* equals x
$\lambda_{IM}(x)$ = mean annual frequency of *IM* exceeding x (ground motion hazard)

A prerequisite to the implementation of Eq. (1) is hazard analysis for a ground motion intensity measure. In this study, the spectral acceleration at the first mode period of the structure, $S_a(T_1)$, is used as the intensity measure. Similar to the *IM* hazard, the mean annual frequency of the *EDP* exceeding a certain value also can be represented in a hazard curve. Two *EDPs* are evaluated: the maximum roof drift and the maximum story drift over the height.

Maximum Drift Hazard Curves

Evaluation of Eq. (1) to compute the the maximum drift hazard (mean annual frequency of drift exceeding y, given that $S_a(T_1)$ equals S_a) requires hazard analysis information on $S_a(T_1)$, which represents the term $\lambda_{IM}(x)$ in Eq. (1), as well as probabilistic data on maximum drift demands. Since this evaluation is performed for structures of a given strength (γ), it is convenient to represent the maximum drift data in the conventional IDA form of $S_a(T_1)$ versus maximum drift, given the strength γ. Representative IDA curves (medians and dispersions) using the maximum roof drift angle, $\theta_{r,max}$, and the maximum story drift angle over the height, $\theta_{s,max}$, for a frame with N = 9, T_1 = 1.8 seconds and γ = 0.1, and various hysteretic models are shown in Fig. 13.

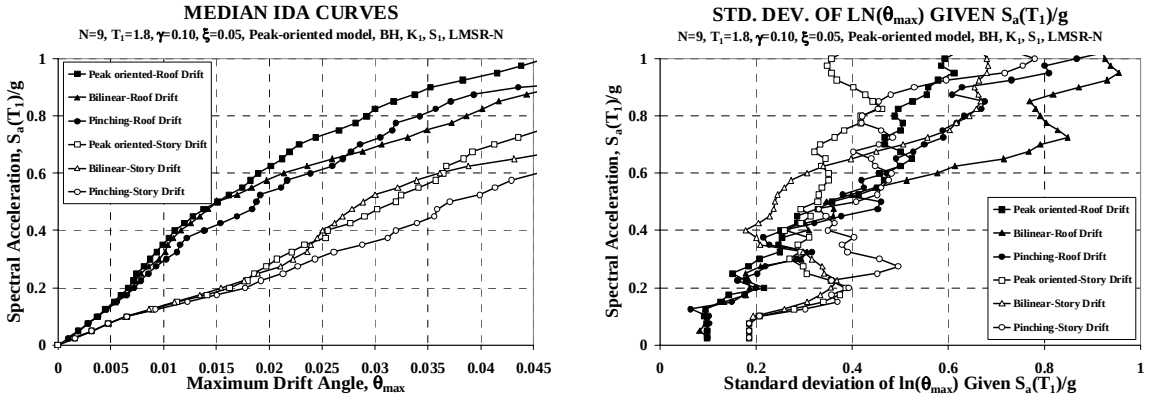

(a) **(b)**

Fig. 13: Incremental dynamic analyses, N = 9, T_1 = 1.8 s., γ = 0.10, various hysteretic models, (a) medians and (b) dispersions

A rigorous evaluation of Eq. (1) can be done by carrying out numerical integration assuming a lognormal distribution of the EDP based on the median and dispersion presented in Fig. 13. However, information on the $S_a(T_1)$ hazard is required to carry out such an evaluation. Based on the work of Cornell et al. [17] the $S_a(T_1)$ hazard can be represented by a curve of the type:

$$\lambda_{S_a(T_1)}(S_a) = P[S_a(T_1) \geq S_a] = k_o S_a^{-k} \tag{2}$$

where the exponent $-k$ approximates the local slope of the hazard curve (in the log domain) around the return period of primary interest.

For illustration of drift hazard curves, an $S_a(T_1)$ hazard curve is utilized that is estimated from the equal-hazard response spectra values calculated for a Van Nuys, CA, site (site class NEHRP D) as part of the PEER research effort to develop Performance-Based Earthquake Engineering Methodologies (Somerville and Collins [18]). At the period of 1.8 sec., and around the hazard level of primary interest (the 10/50 hazard), the following expression for the $S_a(T_1)$ hazard is derived:

$$\lambda_{S_a(1.8)}(S_a) = P[S_a(1.8) \geq S_a] = 0.000373 S_a^{-2.4} \tag{3}$$

Maximum roof and story drift hazard curves computed from numerical integration of Eq. (1) are shown in Fig. 14. The drift hazard curves permit a probabilistic assessment of maximum roof and story drifts, in which the record-to-record variability is considered. For a given mean annual frequency of exceedance of a maximum drift value, the pinching model clearly exhibits the largest maximum roof and story drifts, which is consistent with the general pattern of behavior evaluated in previous sections of this paper.

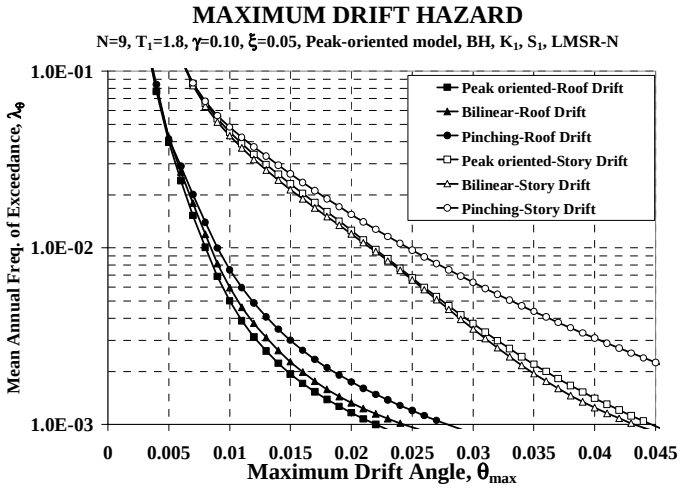

Fig. 14: Maximum drift hazard curves, N = 9, T_1 = 1.8 s., γ = 0.10, various hysteretic models

The conclusion is that a large degree of stiffness degradation does have a noticeable effect on the behavior and the probabilistic seismic performance assessment of regular frames. Thus, an appropriate modeling of the hysteretic behavior at the component level is important in order to carry out reliable seismic performance assessment of existing buildings.

CONCLUSIONS

This paper evaluates the sensitivity of important drift parameters (roof and maximum story drifts) of regular frames to the hysteretic characteristics of the components that control the inelastic response. Three types of hysteretic characteristics at the component level are considered: peak-oriented, bilinear and pinching. Monotonic and cyclic deterioration are not considered; therefore, results are representative of levels of inelastic behavior at with monotonic and cyclic deterioration are not expected to be critical. Moreover, only ordinary ground motions are utilized. Conclusions are to be interpreted within the conditions previously specified.

Results demonstrate that, except for long, flexible frames that are sensitive to P-Delta effects, both the bilinear and the peak-oriented models exhibit similar peak roof and story drift demands regardless of the level of inelastic behavior. In some cases, the peak-oriented model experiences peak drift demands smaller than those experienced by systems with bilinear hysteretic characteristics. However, once significant stiffness degradation is present, e.g., hysteretic behavior represented by the pinching model with small values of κ_d and κ_f, peak roof and story drift demands are clearly larger than those exhibited by the peak-oriented and bilinear models. Moreover, these patterns are more pronounced for MDOF structures than for SDOF systems. For inelastic systems, story drift demands of frames with pinched hysteretic characteristics are particularly larger at the top and at the bottom stories. These patterns of behavior are reflected in the probabilistic seismic demand evaluation of frames as illustrated in the last section of this paper.

The aforementioned patterns are reversed in the case of flexible structures that are sensitive to P-Delta effects. P-Delta sensitive cases are defined as those in which the effect of gravity loads on the deformed configuration of the system causes large displacement amplification in the dynamic response and, sooner or later, dynamic instability. For these cases (e.g., N = 18, T_1 = 3.6 s.), the bilinear model predicts the largest EDPs because the response of the system with bilinear hysteretic behavior spends more time on the envelope of the moment-rotation relationship of its components, which leads to “ratcheting” of the response and potential dynamic instability problems if P-Delta effects produce a negative post-yield tangent stiffness.

The conclusions obtained in this study highlight the importance of:

- A reasonable representation of the hysteretic response of structural elements in MDOF models that are used for seismic response analyses and probabilistic seismic performance assessment.
- The degree of stiffness degradation in the seismic response of regular frames, which is particularly important for the evaluation and rehabilitation of old reinforced-concrete construction.
- The effect of the hysteretic behavior when global collapse due to dynamic instability is of concern.
- Reliable procedures for the identification of “equivalent” or “reference” SDOF systems when they are used to represent the behavior of MDOF structures.

ACKNOWLEDGEMENTS

This research was carried out as part of a comprehensive effort at Stanford's John A. Blume Earthquake Engineering Center to assess seismic demands for frame structures. This effort is supported by the NSF sponsored Pacific Earthquake Engineering Research (PEER) Center. Additional funding was provided by The University of Maryland as part of the faculty start-up package of the first author of this paper. Both sources of support are gratefully acknowledged.

REFERENCES

1. Rahnama M, Krawinkler H. “Effects of soft soil and hysteretic models on seismic demands.” John A. Blume Earthquake Engineering Center Report No. 108, Department of Civil and Environmental Engineering, Stanford University, Stanford, CA, 1993.
2. Oh Y, Han S, Lee L. “Effect of hysteretic models on the inelastic design spectra.” Proceedings of the 12th World Conference on Earthquake Engineering, Auckland, New Zealand. Paper no. 0030, 2000.
3. Song J, Pincheira J. “Spectral displacement demands of stiffness-and strength-degrading systems.” Earthquake Spectra 2000; 16(4): 817-851.
4. Chung S, Loh C. “Identification and verification of seismic demand from different hysteretic models.” Journal of Earthquake Engineering 2002; 6(3): 331-355.
5. Miranda E, Garcia-Ruiz J. “Influence of stiffness degradation on strength demands of structures built on soft soil sites.” Engineering Structures 2002; 24(10): 1271-1281.
6. Farrow K, Kurama Y. “SDOF demand index relationships for performance-based seismic design.” Earthquake Spectra 2003; 19(4): 799-838.
7. Medina RA, Krawinkler H. “Seismic demands for nondeteriorating frame structures and their dependence on ground motions.” John A. Blume Earthquake Engineering Center Report No. 144, Department of Civil and Environmental Engineering, Stanford University, Stanford, CA, 2003.
8. Ibarra LF. “Global collapse of frame structures under seismic excitations.” Ph.D. Dissertation submitted to the Department of Civil and Environmental Engineering, Stanford University, Stanford, CA, 2003.
9. FEMA. “FEMA 368 - NEHRP recommended provisions for seismic regulations for new buildings and other structures.” Federal Emergency Management Agency, Washington D.C, 2000.
10. Prakash V, Powell GH, Campbell S. “DRAIN-2DX: Basic program description and user guide.” Report No. UCB/SEMM-93/17, University of California, Berkeley, CA, 1993.
11. Vamvatsikos D, Cornell CA. “Incremental dynamic analysis.” Earthquake Engineering & Structural Dynamics 2002; 31(3): 491-514.
12. Bernal D. “Instability of buildings subjected to earthquakes.” Journal of Structural Engineering 1992; 118: 2239-2260.
13. Gupta A, Krawinkler H. “Seismic demands for performance evaluation of steel moment resting frame structures.” John A. Blume Earthquake Engineering Center Report No. 132, Department of Civil and Environmental Engineering, Stanford University, Stanford, CA, 1999.
14. Aydinoglu MN. “Inelastic seismic response analysis based on story pushover curves including P-delta effects.” Report No. 2001/1, KOERI, Department of Earthquake Engineering, Bogazici University, Istanbul, 2001.
15. Adam C, Ibarra LF, Krawinkler H. “Evaluation of P-Delta effects in non-deteriorating MDOF structures from equivalent SDOF systems.” Proceedings of the 13th World Conference on Earthquake Engineering, Vancouver, B.C., Canada. Paper no. 3407, 2004.
16. Krawinkler H, Miranda E. “Performance-based earthquake engineering.” Chapter 9 of Earthquake engineering: from engineering seismology to performance-based engineering. CRC Press, 2004.
17. Cornell CA, Jalayer F, Hamburger R, Foutch D. “Probabilistic basis for 2000 SAC Federal Emergency Management Agency steel moment frame guidelines.” ASCE Journal of Structural Engineering 2002; 128(4): 526-534.
18. Somerville P, Collins N. “Ground motion time histories for the Van Nuys building”, PEER Methodology Testbeds Project, URS Corporation, Pasadena, CA, 2002.